



# Selective conditions for the fabrication of a flexible dye-sensitized solar cell with Ti/TiO<sub>2</sub> photoanode

Lu-Yin Lin<sup>a</sup>, Chuan-Pei Lee<sup>a</sup>, R. Vittal<sup>a</sup>, Kuo-Chuan Ho<sup>a,b,\*</sup>

<sup>a</sup> Department of Chemical Engineering, National Taiwan University, Taipei 10617, Taiwan

<sup>b</sup> Institute of Polymer Science and Engineering, National Taiwan University, Taipei 10617, Taiwan

## ARTICLE INFO

### Article history:

Received 2 December 2009

Received in revised form 9 January 2010

Accepted 16 January 2010

Available online 25 January 2010

### Keywords:

Back-illumination

Electrochemical impedance spectroscopy

Flexible dye-sensitized solar cell

Laser-induced photovoltage transients

Ti foil substrate

## ABSTRACT

The effects of four factors, i.e., (i) sputter-deposition time of platinum (Pt) film, (ii) sintering temperature of TiO<sub>2</sub>-coated Ti foil (Ti/TiO<sub>2</sub>), (iii) thickness of Ti foil, and (iv) concentration of iodine are reported for the photovoltaic performance of a back-illuminated flexible dye-sensitized solar cell (DSSC) with Ti foil substrate for the TiO<sub>2</sub> layer. Optimization of these four factors yields a solar-to-electricity conversion efficiency ( $\eta$ ) of 5.95%. Transmittance spectra, cyclic voltammetry (CV), electrochemical impedance spectra (EIS), X-ray diffraction (XRD), scanning electron micrographs (SEM), and laser-induced photovoltage transient technique are used to substantiate the explanations.

© 2010 Elsevier B.V. All rights reserved.

## 1. Introduction

Flexible dye-sensitized solar cells (DSSCs) are convenient for a number of applications especially where cells need complex geometries. Roll to roll production is possible in the case of flexible DSSCs. Poly(ethylene) terephthalate (PET)/indium tin oxide (ITO) is commonly used as the flexible substrate in a DSSC [1–4]. Miyasaka and Kijitori used PET/ITO/TiO<sub>2</sub> as the working electrode and obtained a solar-to-electricity conversion efficiency of 4.1% at 100 mW cm<sup>-2</sup> light intensity for a flexible DSSC [5]. We have previously observed that the cell efficiency increases with the increase of TiO<sub>2</sub>-annealing temperature and becomes saturated at 400–500 °C; this was due to enhanced electron lifetime and increased electron diffusion coefficient for the excited electron in TiO<sub>2</sub> matrix [6]. However, the restriction for the sintering temperature in the case of plastic substrate is still a major problem to be solved. Without sintering at high temperature, the interconnection between TiO<sub>2</sub> particles would be poor and would result in poor performance of the cell. Metal sheet is another choice to fabricate a flexible DSSC, because it can endure very high temperatures. Flexible DSSC using stainless steel as the supporting substrate for working electrode was also developed [7]; to counter the problem of oxide formation

after annealing, a layer of SiO<sub>x</sub> was coated on the stainless steel substrate, followed by deposition of an ITO layer on it to improve its conductivity. Ti, W, and Zn were also studied as substrates for working electrodes [8,9]. Lin et al. fabricated a DSSC using a conical-shaped anodic TiO<sub>2</sub>-nanotube (TiNT)/Ti and obtained a conversion efficiency ( $\eta$ ) of 4.3%, under AM1.5 with back side illumination [10]. The highest ever efficiency of 7.2% was achieved for a flexible DSSC by using Ti foil as the working electrode [11].

We used in this work a Ti foil as the substrate for the working electrode in a DSSC, with the awareness that its sheet resistance is higher than those of other metal substrates, such as silver and copper. Ti has higher conductivity, compared to that of transparent conducting oxide (TCO) substrate. Moreover, Ti has superior corrosion resistance due to the existence of a passive film of TiO<sub>2</sub> on it.

In this paper, we present the effects of sputter-deposition time of Pt, sintering temperature of TiO<sub>2</sub>-coated Ti foil, thickness of Ti foil, and the concentration of I<sub>2</sub> on the photovoltaic performance of a flexible DSSC. Owing to the formation of oxide on Ti substrate, the study pertaining to sintering temperature of TiO<sub>2</sub>-coated Ti became necessary and is different from that of a bare TiO<sub>2</sub> film. To the best of our knowledge, these aspects were not studied for a flexible DSSC with Ti as the substrate for the photoanode. Optimizing these conditions, we obtained a solar-to-electricity conversion efficiency of 5.95%, which is one of the best for a cell with Ti metal. Study on photovoltaic parameters of DSSCs, with time-dependent sputtered Pt layers, characterization of such layers through transmission spectra, characterization of Ti/TiO<sub>2</sub> films through XRD, SEM

\* Corresponding author at: Department of Chemical Engineering, National Taiwan University, No. 1, Sec. 4, Roosevelt Rd., Taipei 10617, Taiwan. Tel.: +886 2 2366 0739; fax: +886 2 2362 3040.

E-mail address: [kcho@ntu.edu.tw](mailto:kcho@ntu.edu.tw) (K.-C. Ho).

and laser-induced photovoltage transients, study on the effects of  $I_2$  concentration on the photovoltaic parameters of a Ti-based flexible DSSC are novel aspects of this research.

## 2. Experimental

Lithium iodide (LiI), iodine ( $I_2$ ), and poly(ethylene glycol) (PEG, M.W. = 20,000) were obtained from Merck; 4-tert-butylpyridine (TBP) and tert-butyl alcohol were obtained from Acros. Titanium (IV) tetraisopropoxide (TTIP), acetonitrile, acetylacetone, ethanol, and isopropyl alcohol (IPA) were obtained from Aldrich. 1,2-Dimethyl-3-propylimidazolium iodide (DMPII) was obtained from Solaronix. 3-Methoxypropionitrile (MPN) was obtained from Fluka.

Commercial titanium dioxide (ST-21,  $50 \text{ m}^2 \text{ g}^{-1}$ , 6 g, Ya Chung Industrial Co. Ltd., Taiwan) was thoroughly mixed with a solution of acetylacetone ( $500 \mu\text{l}$ ) in DI-water (11 g). This was stirred for 3 days and 1.8 g of PEG was then added to the well-dispersed colloidal solution. The mixture was stirred for an additional 2 days to prepare the required  $TiO_2$  paste. Ti foil (Fuu Cherng Co. Ltd., Taiwan) was first cleaned with a neutral cleaner, and then washed with DI-water, acetone, and IPA, sequentially. Surface of the Ti foil was treated with a solution of TTIP (0.028 g) in ethanol (10 ml) for obtaining a good mechanical contact between the metal Ti foil and the  $TiO_2$  film. From the  $TiO_2$  paste a thin film ( $10 \mu\text{m}$ ) of  $TiO_2$  was then coated onto the treated Ti foil by using the doctor blade technique; a portion of  $0.4 \times 0.4 \text{ cm}^2$  was selected as the active area by removing the side portions by scraping. The thus obtained  $TiO_2$  film was gradually heated to various high temperatures (350, 400, 450 and  $500^\circ\text{C}$ ) in an oxygen atmosphere, and sintered at each of these temperatures for 30 min. After cooling to  $80^\circ\text{C}$ , the Ti/ $TiO_2$  electrode was immersed in a  $3 \times 10^{-4} \text{ M}$  solution of *cis*-di(thiocyanato)-*N,N'*-bis(2,2'-bipyridyl-4-carboxylic acid-4'-tetrabutylammonium carboxylate)ruthenium(II) (N719, Solaronix S.A., Aubonne, Switzerland) in acetonitrile and tert-butyl alcohol (volume ratio of 1:1) at room temperature for 24 h. Meanwhile transparent Pt counter electrodes (CEs) were prepared by sputtering Pt on polyethylene naphthalate (PEN)/ITO ( $Al_2O_3$  coated,  $<13 \Omega \text{ sq.}^{-1}$ ) for 10, 20, 30, 55, 80, 130, and 180 s (under a sputter current of 20 mA). The dye-coated  $TiO_2$  foil was then assembled with a Pt-CE; the two electrodes were sealed with a hot-melt gasket of  $25 \mu\text{m}$  thickness made of the ionomer Surlyn (SX1170-25, Solaronix S.A., Aubonne, Switzerland) and sealed by heating. The electrolyte consisted of a mixture of 0.1 M LiI, 0.6 M DMPII, 0.5 M TBP, and various amounts of  $I_2$  in MPN. The electrolyte was injected into the gap between the electrodes by capillarity. For this injection purpose a hole was previously made in the CE with a drilling machine. After the electrolyte-injection, the hole was sealed with hot-melt glue.

The flexible DSSC was illuminated by a class A quality solar simulator (PEC-L11, AM1.5G, Peccell Technologies, Inc.) from the side of PEN/ITO/Pt and the incident light intensity ( $100 \text{ mW cm}^{-2}$ ) was calibrated with a standard Si Cell (PECSI01, Peccell Technologies, Inc.). The photoelectrochemical characteristics of a DSSC were recorded with a potentiostat/galvanostat (PGSTAT 30, Autolab, Eco-Chemie, the Netherlands). The film thickness was determined using a surface profilometer (Sloan Dektak 3030). X-ray diffraction patterns (XRD, MO3XHF, MAC) were obtained to analyze the crystal phases of a  $TiO_2$  film. In addition, the thickness of the metal oxide on Ti foil working electrode was observed by a scanning electron microscope (SEM, LEO 1530, LEO Electron Microscopy). UV-vis spectrophotometer (V-570, Jasco, Japan) and cyclic voltammetry (CV) were respectively used to investigate the transmittance properties and the catalytic abilities of the Pt-CEs. Electrochemical impedance spectra (EIS) were obtained by the above-mentioned potentiostat/galvanostat equipped with an FRA2 module, under a

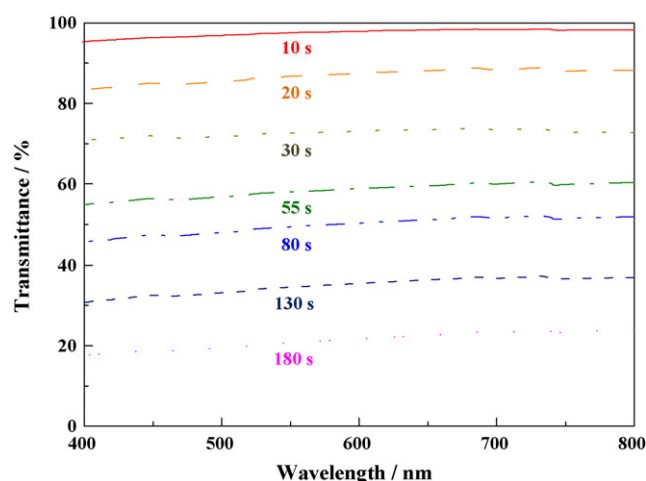


Fig. 1. Transmittance spectra obtained with Pt-CEs with different deposition times of Pt layers (baseline with bare ITO electrode).

constant light illumination of  $100 \text{ mW cm}^{-2}$ . The frequency range explored was 10 mHz to 65 kHz. The applied bias voltage was set at the open-circuit voltage of the DSSC, between the PEN/ITO/Pt-CE and the FTO/ $TiO_2$ /dye working electrode, starting from the short-circuit condition; the corresponding ac amplitude was 10 mV. The impedance spectra were analyzed using an equivalent circuit model [12,13]. Pulsed laser excitation was applied by a frequency-doubled Q-switched Nd:YAG laser (model Quanta-Ray GCR-3-10, Spectra-Physics laser) with a 2 Hz repetition rate at 532 nm, and a 7 ns pulse width at half-height. The average electron lifetime could be approximately estimated by fitting a decay of the open-circuit voltage transient with  $\exp(-t/\tau_e)$ , where  $t$  is the time and  $\tau_e$  is an average time constant before recombination.

## 3. Results and discussion

In the case of a metal-based working electrode in a flexible DSSC, the illumination should be done from the back side due to the non-transparent nature of the metal substrate; considering this aspect, the CE of such a cell assumes great importance. These types of CEs should have the following characteristics: (1) high conductivity for transporting electrons, (2) excellent catalytic activity for triiodide reduction, and (3) high transparency for the penetration of light through the electrode.

In this study, the Pt-CEs were prepared by sputtering Pt on PEN/ITO substrates, and the deposition times were varied from 10 to 180 s. As shown in Fig. 1, the transmittance of a Pt-CE decreases with the increase of the Pt deposition time, especially in the range from 400 to 700 nm. Although high transparent Pt-CE is favorable for a back-illuminated DSSC, its catalytic ability is also to be taken into account from the viewpoint of efficiency of the cell. Fig. 2 shows overlaid CVs recorded for various deposition times of Pt on the CEs. The absolute cathodic peak current ( $I_{pc}$ ) of a CV represents the electrochemical activities of a Pt-CE [14]. The absolute  $I_{pc}$ 's of the CVs show increases with increasing deposition times of Pt until 30 s, and the peak currents remain almost the same with further deposition times. These results suggest that the catalytic ability of a Pt layer for  $I_3^-$  reduction increases with the increase of deposition time up to 30 s, and then remains the same with further deposition times. The CE with the bare ITO shows an  $I_{pc}$  value close to zero, revealing that it has no catalytic ability for the reduction of  $I_3^-$ .

Fig. 3 shows photovoltaic performances of DSSCs with different deposition times of Pt layers, measured at  $100 \text{ mW cm}^{-2}$  light intensity and illuminated from the CE side. Table 1 gives the corresponding open-circuit voltage ( $V_{oc}$ ), short-circuit current density

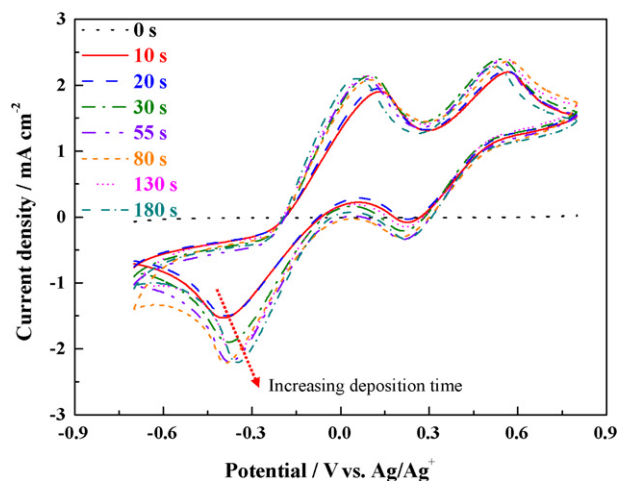


Fig. 2. Cyclic voltammograms obtained with Pt-CEs with different deposition times of Pt layers (bare ITO electrode shows zero current).

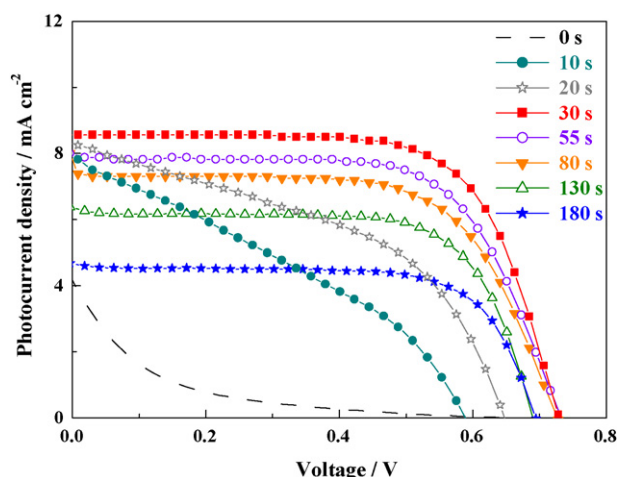


Fig. 3. Photocurrent–voltage characteristics of DSSCs with different deposition times of Pt layers, measured at  $100 \text{ mW cm}^{-2}$  light intensity and illuminated from the CE side.

( $J_{sc}$ ), fill factor (FF) and cell efficiency ( $\eta$ ) for DSSCs with different Pt deposition times. The  $J_{sc}$  value increases with increasing deposition time up to 30 s and decreases with further deposition time. For the deposition times from 30 to 180 s, the continuous decrease of  $J_{sc}$  may be attributed to the decrease in transmittance with increasing Pt thickness. On the other hand, the lesser values of  $J_{sc}$  for deposition times lesser than 30 s may be attributed to the insufficient catalytic ability of the Pt layers, notwithstanding their higher transmittance. When the sputtering time is less than 30 s, the cell performance decreased dramatically. The best

Table 1

Photovoltaic parameters and electrochemical impedance data of the DSSCs with different deposition times of Pt layers, measured at  $100 \text{ mW cm}^{-2}$  light intensity and illuminated from the CE side.

Deposition time (s)	$V_{oc}$ (V)	$J_{sc}$ ( $\text{mA cm}^{-2}$ )	FF	$\eta$ (%)	$R_{ct1}$ ( $\Omega$ )	$R_{ct2}$ ( $\Omega$ )
0	0.68	1.86	0.07	0.09	–	–
10	0.59	7.75	0.35	1.58	28.26	41.25
20	0.65	8.25	0.46	2.48	21.05	40.87
30	0.73	8.56	0.70	4.33	10.35	41.33
55	0.73	7.88	0.68	3.91	10.02	50.14
80	0.72	7.31	0.67	3.56	11.12	52.68
130	0.70	6.19	0.71	3.06	11.03	63.62
180	0.70	4.56	0.71	2.29	11.34	69.86

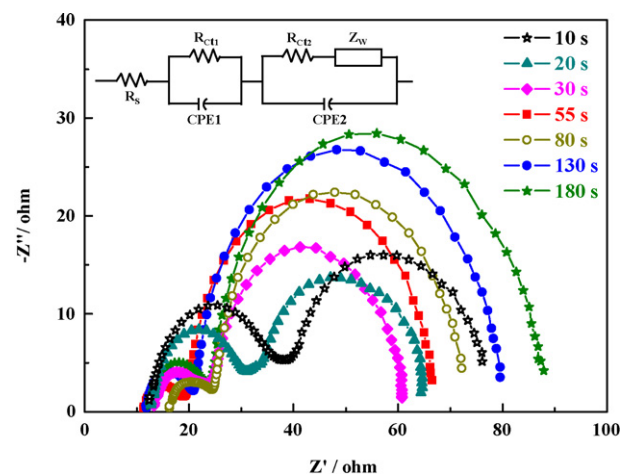
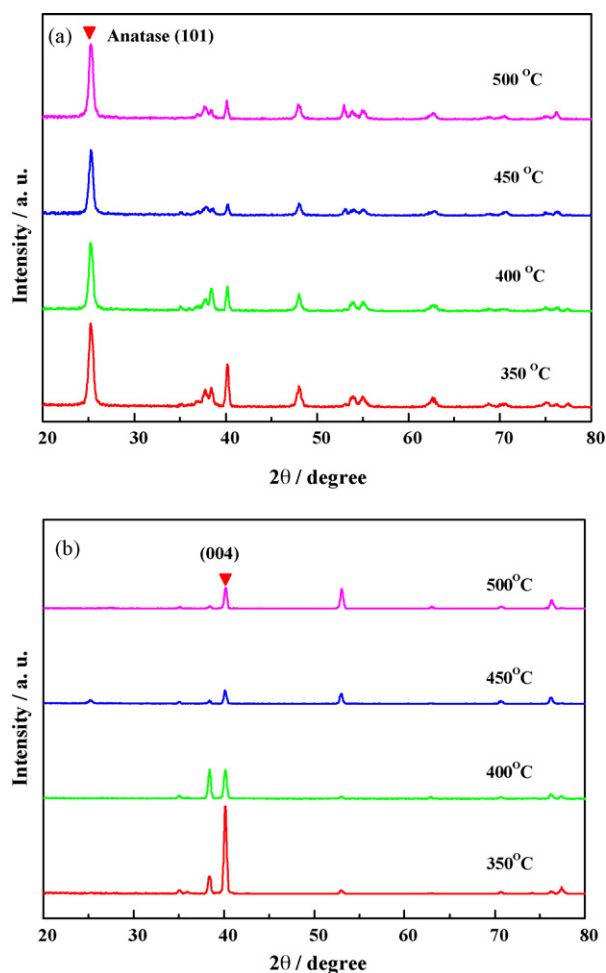


Fig. 4. Electrochemical impedance spectra of the DSSCs with different deposition times of Pt layers, measured at  $100 \text{ mW cm}^{-2}$  light intensity under open-circuit voltage. The frequency range was 10 mHz to 65 kHz.

cell efficiency of 4.33% was achieved with a sputtering time of 30 s.

EIS technique was used to study the charge transfer resistances of the cells, which were in consistency with the results obtained from the photovoltaic characteristics. Fig. 4 illustrates the EIS data of the solar cells with various deposition times of the Pt layers. The equivalent circuit is shown in the inset of Fig. 4. The ohmic serial resistance ( $R_s$ ) in the equivalent circuit corresponds to the overall series resistance. In general, the impedance spectrum of a DSSC shows three semicircles in the frequency range of 10 mHz to 65 kHz. The first, second and third semicircles correspond to the charge transfer resistances at the CE ( $R_{ct1}$ ), at the  $\text{TiO}_2/\text{dye}/\text{electrolyte}$  interface ( $R_{ct2}$ ) and to the Warburg diffusion process of  $\text{I}^-/\text{I}_3^-$  in the electrolyte ( $R_{diff}$ ), respectively. A very thin spacer was used in our device. Therefore, the  $R_{diff}$  is not obvious, and it is overlapped by  $R_{ct2}$ . The corresponding values of  $R_{ct1}$  and  $R_{ct2}$  are showed in Table 1. The  $R_{ct1}$  shows decreases with increases in deposition time until 30 s which can be attributed to the enhancement of catalytic ability of the Pt layers, and it ( $R_{ct1}$ ) maintains almost the same value for further deposition, which indicates that the catalytic ability is the same with deposition time of more than 30 s. On the other hand, with lesser deposition times (<30 s), the transmittance is higher for light to cause enough dye to be excited. Therefore there is not much difference in  $R_{ct2}$  values with Pt deposition times of lesser than 30 s. It can also be seen in Fig. 4 that the longer the deposition time of a Pt layer, the larger the charge transfer resistance at the  $\text{TiO}_2/\text{dye}/\text{electrolyte}$  interface ( $R_{ct2}$ ); this observation is in consistency with the corresponding decreased values of  $J_{sc}$  (Table 1).

It is known that the crystal phase of a  $\text{TiO}_2$  film can be varied by varying the sintering temperature and its preparation method [15]. In order to characterize the crystal phase of the  $\text{TiO}_2$ , sintered at 350, 400, 450 and 500 °C, XRD was applied. Fig. 5(a) and (b) shows, respectively the XRD patterns of  $\text{TiO}_2$  film and Ti foil sintered separately at various temperatures. The XRD pattern of  $\text{TiO}_2$  film shows a peak corresponding to (1 0 1) of the  $\text{TiO}_2$  structure, which is associated with the anatase phase, and this peak is the same for various sintering temperatures, whereas the peak corresponding to (0 0 4) of Ti foil decreased with higher sintering temperatures. The cross-sectional image of the sintered Ti foil was observed by means of scanning electron microscopy (SEM) and is shown in Fig. 6; it can be seen in the figure that the thickness of metal oxide increases with increasing sintering temperature, which is undesirable, because the transport of electrons would be adversely affected due to the formation of metal oxide.



**Fig. 5.** X-ray diffraction patterns of (a)  $\text{TiO}_2$  film and (b) Ti foil, obtained after sintering them separately at different temperatures.

**Table 2**

Photovoltaic parameters of the DSSCs with their Ti/TiO<sub>2</sub> sintered at different temperatures, measured at 100 mW cm<sup>-2</sup>, the table also shows the electron lifetimes in corresponding TiO<sub>2</sub>'s.

Temperature (°C)	$V_{OC}$ (V)	$J_{SC}$ (mA cm <sup>-2</sup> )	FF	$\eta$ (%)	$\tau_e$ (ms)
350	0.71	7.38	0.72	3.77	16.38
400	0.73	8.06	0.70	4.09	17.13
450	0.73	8.56	0.70	4.33	18.56
500	0.73	8.31	0.68	4.10	17.63

Table 2 gives the photovoltaic parameters of DSSCs with TiO<sub>2</sub>-coated Ti foils sintered at different sintering temperatures, measured at 100 mW cm<sup>-2</sup> light intensity. It shows that the highest efficiency of 4.33% was achieved with 450 °C as the sintering temperature. The  $J_{SC}$  increased with increasing sintering temperature up to 450 °C and then decreased with further annealing. We assume that improvement of interconnection between particles with increasing sintering temperature is the cause for the initial increase of  $J_{SC}$  and formation of excessive metal oxide is the cause for slight decrease of  $J_{SC}$  at 500 °C. The effect of sintering temperature of a Ti/TiO<sub>2</sub> film on the average electron lifetime ( $\tau_e$ ) in the corresponding TiO<sub>2</sub> was studied by a laser-induced photovoltage transient technique, and the results are shown in Fig. 7. The average electron lifetime can approximately be estimated by fitting a decay of the open-circuit voltage transient with  $\exp(-t/\tau_e)$ , where  $t$  is the time and  $\tau_e$  is an average time constant before recombination. The values of  $\tau_e$  of the TiO<sub>2</sub> films were found to be 16.38,

**Table 3**

Photovoltaic parameters of the DSSCs with Ti foils of different thicknesses, measured at 100 mW cm<sup>-2</sup>.

Thickness (mm)	$V_{OC}$ (mV)	$J_{SC}$ (mA cm <sup>-2</sup> )	FF	$\eta$ (%)
0.40	0.76	10.31	0.70	5.50
0.25	0.75	9.48	0.69	4.90
0.10	0.73	8.56	0.70	4.33
0.05	0.71	8.13	0.72	4.16

**Table 4**

Photovoltaic parameters of the DSSCs with different I<sub>2</sub> concentrations, measured at 100 mW cm<sup>-2</sup>, conductivities of the corresponding electrolytes are also shown in the last column.

Concentration of I <sub>2</sub> (M)	$V_{OC}$ (V)	$J_{SC}$ (mA cm <sup>-2</sup> )	FF	$\eta$ (%)	$\sigma_s$ (mS cm <sup>-1</sup> )
0.01	0.78	8.38	0.59	3.85	9.3
0.02	0.76	10.69	0.63	5.07	11.5
0.03	0.74	10.25	0.68	5.19	13.7
0.04	0.76	11.69	0.67	5.95	14.4
0.05	0.76	10.31	0.70	5.50	16.0
0.06	0.76	9.44	0.68	4.89	17.2
0.07	0.76	8.94	0.69	4.69	17.7

17.13, 18.56 and 17.63 ms for TiO<sub>2</sub> electrodes sintered at 350, 400, 450, and 500 °C, respectively. The figure shows the largest values of  $\tau_e$  for the Ti/TiO<sub>2</sub> film sintered at 450 °C, which implies that the collection and transport of electrons will be at best when the Ti/TiO<sub>2</sub> film is sintered at 450 °C.

To investigate the effects of thickness of Ti foil as working electrode substrate on the cell performance, Ti foils with four different thicknesses (0.40, 0.25, 0.10, and 0.05 mm) were used. Table 3 lists the corresponding values of  $V_{OC}$ ,  $J_{SC}$ , FF and  $\eta$ . The highest efficiency of 5.50% was obtained with the thickest Ti foil (0.4 mm). The  $J_{SC}$  increases with increasing thickness, which is the result of decreased resistance of the Ti foil with its increased thicknesses. According to the law of resistances, conductor's resistance is directly proportional to its length and inversely proportional to its cross-sectional area. Consequently, with the largest cross-sectional area, the thickest Ti foil has the lowest resistance than other Ti foils. Ti foil thicker than 0.4 mm cannot be used as working substrate, as it becomes inflexible, which hampers the basic idea of our research to fabricate a flexible DSSC.

It is well known that I<sub>2</sub> exists in the electrolyte with iodides in the form of polyiodides such as I<sub>3</sub><sup>-</sup> or I<sub>5</sub><sup>-</sup>. An efficient transport of iodide and triiodide in the electrolyte is necessary for the good performance of a DSSC, because the oxidized dye should be regenerated by I<sup>-</sup> efficiently after the electrons from the excited state of the dye are injected into the conduction band of TiO<sub>2</sub> under illumination. At the same time, the electrons accumulated at the CE through the external circuit will lead to concentration overpotentials for the electrolyte at the CE and loss of energy for the DSSC, if the electrons are not transferred from the CE to I<sub>3</sub><sup>-</sup> efficiently. However, an increasing content of I<sub>2</sub> (or I<sub>3</sub><sup>-</sup>) leads to enhanced light absorption by the electrolyte even in the visible range [16]. In addition, excessive I<sub>2</sub> would increase the dark reduction current. Therefore, an optimized ratio of I<sub>2</sub>/LiI is necessary to achieve perfection for a DSSC.

Table 4 presents photovoltaic parameters of the DSSCs with different concentrations of I<sub>2</sub> in their electrolytes; the table also shows the ionic conductivities of the corresponding electrolytes. The best cell efficiency of 5.95% was obtained for the DSSC with 0.04 M of I<sub>2</sub> in the electrolyte.

The  $J_{SC}$  increases with the increase of I<sub>2</sub> concentration up to 0.04 M, and further increase in I<sub>2</sub> concentration decreases the  $J_{SC}$  of the cells. The initial increase in  $J_{SC}$  is due to increasing ionic conductivity with increasing concentration of I<sub>2</sub>, and the subsequent decrease in the  $J_{SC}$  is because of the increase in recombination rate.

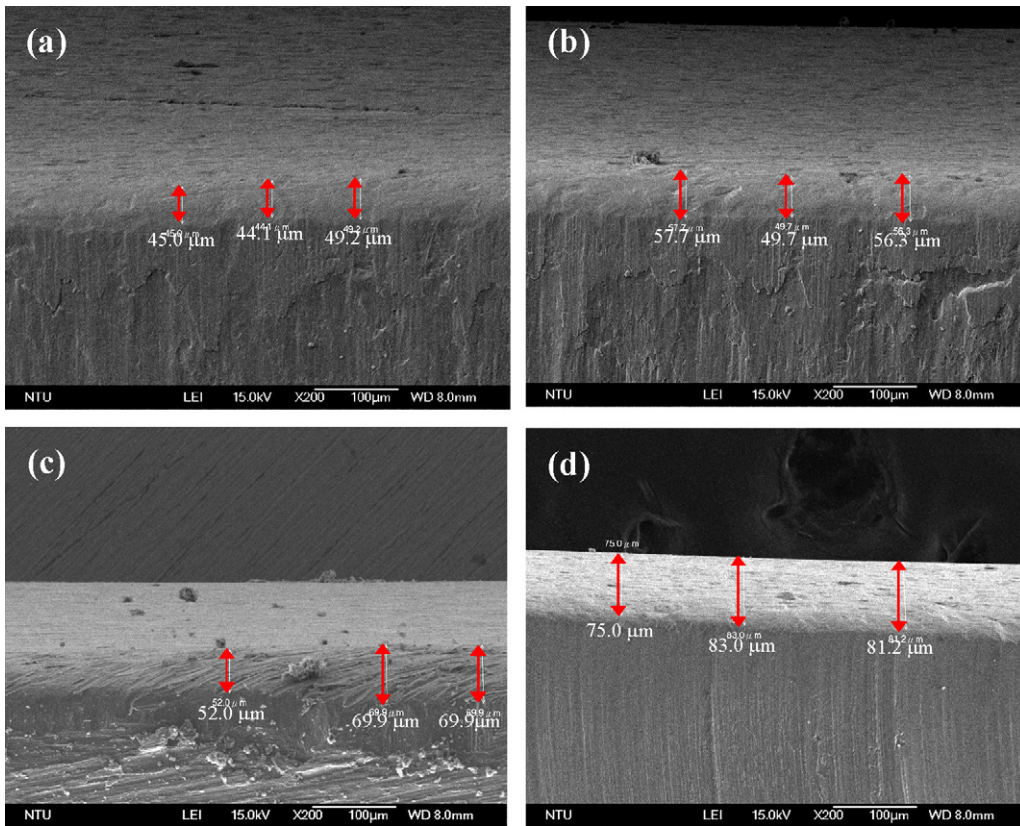


Fig. 6. Cross-section SEM images of Ti foils sintered at (a) 350 °C, (b) 400 °C, (c) 450 °C, and (d) 500 °C.

The ionic conductivities ( $\sigma_S$ ) of the electrolytes at different concentrations of  $I_2$  were determined using the following formula:

$$\sigma_S = d_S / (A_S \times R_S) \tag{1}$$

The ohmic serial resistance ( $R_S$ ) in the formula was obtained from Nyquist plot (Pt/electrolyte/Pt), and the device constants ( $d_S$  and  $A_S$ ) were calculated from a standard cell calibration based on a NaCl solution of  $12.9 \text{ mS cm}^{-1}$  (Model 011006, Thermo Orion). It can be seen in the table that the ionic conductivity increases with the increase in the concentration of  $I_2$ . Fig. 8 illustrates the dark currents of the DSSCs with different concentrations of  $I_2$  in their electrolytes. Apparently, the dark current density increases with increasing iodine concentration, which means the increasing recombination rate as well.

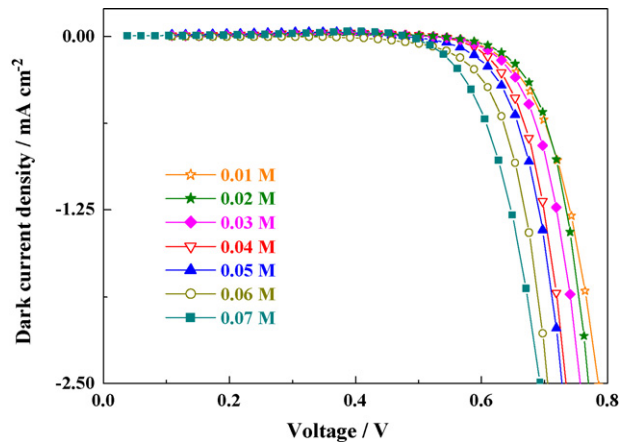


Fig. 8. Dark current densities of the DSSCs with different  $I_2$  concentrations in their electrolytes.

#### 4. Conclusion

A study was made on the effects of sputter-deposition time of Pt film, sintering temperature of  $TiO_2$ -coated Ti foil, thickness of Ti foil, and concentration of iodine on the photovoltaic performance of a flexible DSSC, fabricated with Ti foil and PEN/ITO as the substrates for working and CE, respectively. The following conclusions are made:

- (a) Solar to electricity efficiency ( $\eta$ ) increases with increasing deposition time of Pt up to 30 s and then decreases with further increase in deposition time.
- (b)  $\eta$  increases with increasing sintering temperature up to 450 °C and then slightly decreases at 500 °C.

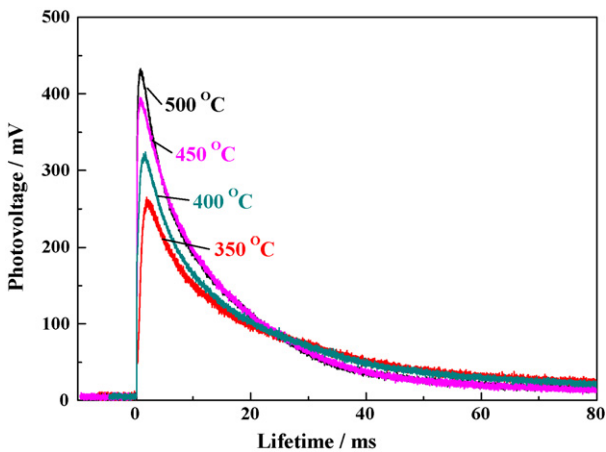


Fig. 7. Transient photovoltage curves of the DSSCs with their Ti/ $TiO_2$ 's sintering at different temperatures.

- (c)  $\eta$  increases with increasing thickness of Ti foil from 0.05 to 0.40 mm.
- (d)  $\eta$  increases with increasing concentration of  $I_2$  in the electrolyte up to 0.04 M and then decreases with further increase in  $I_2$  concentration.
- (e) Transmittance of a sputter-deposited Pt-CE decreases with increase of sputtering time.
- (f) Catalytic ability of a sputter-deposited Pt layer for  $I_3^-$  reduction increases with the increase of deposition time up to 30 s, and then remains the same with further deposition times.
- (g) ITO glass has no catalytic ability for the reduction of  $I_3^-$  ions.
- (h) In the case of a flexible DSSC with Ti metal as the substrate for working electrode, the collections and transport of electrons will be at their best, when the Ti/TiO<sub>2</sub> film is sintered at 450 °C.
- (i) Recombination rate increases in a flexible DSSC of the type in this study with increasing iodine concentration.

The crystal phases of TiO<sub>2</sub> were found to be almost the same for sintering temperatures of up to 500 °C, and Ti showed increased formation of corresponding oxide with increasing temperature. After optimization of the above-mentioned factors, the highest efficiency of 5.95% was achieved for the optimized DSSC. The best cell showed reduced charge transfer resistance, reduced recombination reactions, and increased electron lifetime in its TiO<sub>2</sub> film, in consistency with its high efficiency.

#### Acknowledgements

This work was supported in part by the National Research Council of Taiwan. Some of the instruments used in this study were made

available through the financial support of the Academia Sinica, Taipei, Taiwan, under grant AS-97-TP-A08.

#### References

- [1] M. Tomiha, S. Uchida, H. Takizawa, M. Kawaraya, *Sol. Energy Mater. Sol. Cells* 81 (2004) 135–139.
- [2] M. Tomiha, S. Uchida, N. Masaki, A. Miyazawa, H. Takizawa, *J. Photochem. Photobiol. A: Chem.* 164 (2004) 93–96.
- [3] M. Durr, A. Schmid, M. Obermaier, S. Rosselli, A. Yasuda, G. Nelles, *Nat. Mater.* 4 (2005) 607–611.
- [4] D.S. Zhang, T. Yoshida, T. Oekermann, K. Furuta, H. Minoura, *Adv. Funct. Mater.* 16 (2006) 1228–1234.
- [5] T. Miyasaka, Y. Kijitori, *J. Electrochem. Soc.* 151 (2004) A1767–A1773.
- [6] K.M. Lee, V. Suryanarayanan, K.C. Ho, *Sol. Energy Mater. Sol. Cells* 91 (2007) 1416–1420.
- [7] M.G. Kang, N.G. Park, K.S. Ryu, S.H. Chang, K.J. Kim, *Sol. Energy Mater. Sol. Cells* 90 (2006) 574–581.
- [8] M.G. Kang, N.G. Park, K.S. Ryu, S.H. Chang, K.J. Kim, *Chem. Lett.* 34 (2005) 804–805.
- [9] Y. Jun, M.G. Kang, *J. Electrochem. Soc.* 154 (2007) B68–B71.
- [10] C.J. Lin, W.Y. Yu, S.H. Chien, *Appl. Phys. Lett.* 93 (2008) 133107-1–133107-3.
- [11] S. Ito, N.L.C. Ha, G. Rothenberger, P. Liska, P. Comte, S.M. Zakeeruddin, P. Pechy, M.K. Nazeeruddin, M. Grätzel, *Chem. Commun.* 38 (2006) 4004–4006.
- [12] L. Han, N. Koide, Y. Chiba, T. Mitate, *Appl. Phys. Lett.* 84 (2004) 2433–2435.
- [13] L. Han, N. Koide, Y. Chiba, A. Islam, T. Mitate, C. R. Chimie 9 (2006) 645–651.
- [14] W. Kubo, S. Kambe, S. Nakade, T. Kitamura, K. Hanabusa, Y. Wada, S. Yanagida, *J. Phys. Chem. B* 107 (2003) 4374–4381.
- [15] S. Nakade, M. Matsuda, S. Kambe, Y. Saito, T. Kitamura, T. Sakata, Y. Wada, H. Mori, S. Yanagida, *J. Phys. Chem. B* 106 (2002) 10004–10010.
- [16] A.I. Popov, R.F. Swensen, *J. Am. Chem. Soc.* 77 (1955) 3724–3726.